J|A|C|S
ARTICLES

Published on Web 02/19/2010

CO_2 Binding by Dynamic Combinatorial Chemistry: An Environmental Selection

Julien Leclaire,*,† Guillaume Husson,† Nathalie Devaux,† Vincent Delorme,† Laurence Charles,‡ Fabio Ziarelli,§ Perrine Desbois,⊥ Alexandra Chaumonnot,⊥ Marc Jacquin,⊥ Frédéric Fotiadu,*,† and Gérard Buono†

Laboratoire Chirosciences, UMR 6263 CNRS: Institut des Sciences Moléculaires de Marseille ISM2, École Centrale Marseille, Université Paul Cézanne, case A62, Avenue Escadrille Normandie-Niemen, 13397 Marseille Cedex 20, France, Universités Aix-Marseille I, II, and III - CNRS, UMR 6264: Laboratoire Chimie, Provence, Spectrométries Appliquées à la Chimie Structurale, F-13397 Marseille, France, Aix-Marseille Université, Fédération des Sciences Chimiques, Spectropôle, case 511, avenue Escadrille Normandie Niémen, 13397 Marseille cedex 20, France, and IFP, IFP-Lyon, BP no. 3, 69360 Solaize, France

Received December 3, 2009; E-mail: julien.leclaire@centrale-marseille.fr; frederic.fotiadu@centrale-marseille.fr

Abstract: We now report that a dynamic combinatorial selection approach can quantitatively provide, from trivial building blocks, an architecturally complex organic material, in which carbon dioxide is reversibly but covalently incorporated as a guest with a mass content of 20%. Solid-state analyses combined with covalent disconnection and quantization of the liberated components allowed identification of a three-component monomeric unit repeated within a range of assembled oligomeric adducts whose repartition and binding capacity can be finely tuned through the starting stoichiometries. The self-assembly of these architectures occurs through the simultaneous creation of more than 25 covalent bonds per molecular entity. It appears that the thermodynamic selection is directed by the packing efficiency of these adducts, explaining the spectacular building block discrimination between homologues differing by one carbon unit. This selectivity, combined with the reversible nature of the system, provided pure molecular building blocks after a simple chemical disconnection, promoting CO_2 as a green auxiliary to purify polyaldehyde or polyamine from mixtures of homologous structures. Moreover, the gas template could be expelled as a pure compound under thermodynamic control. This cooperative desorption process yielded back the initial libraries of high molecular diversity with a promising reduction of the energetic costs of capture and recycling.

Introduction

Primary and secondary amines can reversibly trap carbon dioxide through the formation of ammonium carbamates, a simple, quick and reversible reaction for CO_2 transportation during the respiratory process.[1] This strategy is also used by industrial units devoted to gaseous streams purification[2] and is explored in pilot installations[3] aimed at reducing anthropic emissions. Among reversible reactions explored in chemistry, few involve a gaseous entity at room temperature.[4] According to Le Chatelier's rules, the covalent carbamate linkage, albeit robust and stable,[5] can release CO_2 and the initial amines upon gentle heating and/or reduction of partial pressure. Carbon dioxide therefore meets all requirements to be used, through ammonium carbamate formation, as a reversible, green and cheap agent for introducing ion pairs and hydrogen bonds into molecular systems. A chaotic assembly of initially independent molecules can indeed be organized, through ammonium carbamate pairing, into a network of controlled extension with original and thermally reversible macroscopic properties, such as ionic liquids,[6] hybrid materials,[7] organogels,[8] or supramolecular polymers.[9]

In an effort to create tailored molecular receptors for CO_2, we turned to dynamic combinatorial chemistry (DCC)[10] as a

† Université P. Cézanne, École Centrale Marseille - CNRS, UMR 6263.
‡ Universités Aix-Marseille I, II, and III - CNRS, UMR 6264.
§ Aix-Marseille Université, Fédération des Sciences Chimiques, Spectropôle.
⊥ Institut Francais du Petrole, Separation.

(1) (a) Arnone, A. *Nature* **1974**, *247*, 143–145. (b) Luzzana, M.; Marre, C.; Perrella, M.; Rossi-Bernardi, L.; Roughton, F. J. *J. Physiol.* **1972**, *224*, P65–66.
(2) Kohl, A.; Nielsen, R. *Gas Purification*, 5th ed.; Gulf Publishing: Houston, 1997.
(3) Notz, R.; Asprion, N.; Clausen, I.; Hasse, H. *Chem. Eng. Res. Des.* **2007**, *85*, 510–515.
(4) (a) Rudkevich, D. M.; Xu, H. *Chem. Commun.* **2005**, 2651–2659. (b) Rudkevich, D. M. *Eur. J. Org. Chem.* **2007**, 3255–3270.
(5) Dell'Amico, D. B.; Calderazzo, F.; Labella, L.; Marchetti, F.; Pampaloni, G. *Chem. Rev.* **2003**, *103*, 3857–3897.
(6) (a) Bates, E. D.; Mayton, R. D.; Ntai, I.; Davis, J. H., Jr. *J. Am. Chem. Soc.* **2004**, *124*, 926–927. (b) Liu, Y.; Jessop, P. G.; Cunningham, M.; Eckert, C. A.; Liotta, C. L. *Science* **2006**, *313*, 958–960. (c) Jessop, P. G.; Heldebrant, D. J.; Li, X.; Eckert, C. A.; Liotta, C. L. *Nature* **2005**, *436*, 1102.
(7) Alauzun, J.; Mehdi, A.; Reyé, C.; Corriu, R. J. P. *J. Am. Chem. Soc.* **2005**, *127*, 11204–11205.
(8) Georges, M.; Weiss, R. G. *Langmuir* **2002**, *18*, 7124–7135.
(9) (a) Xu, H.; Rudkevich, D. M. *Chem.—Eur. J.* **2004**, *10*, 5432–5442. (b) Stastny, V.; Rudkevich, D. M. *J. Am. Chem. Soc.* **2007**, *129*, 1018–1019.

 10.1021/ja909975q © **2010 American Chemical Society**

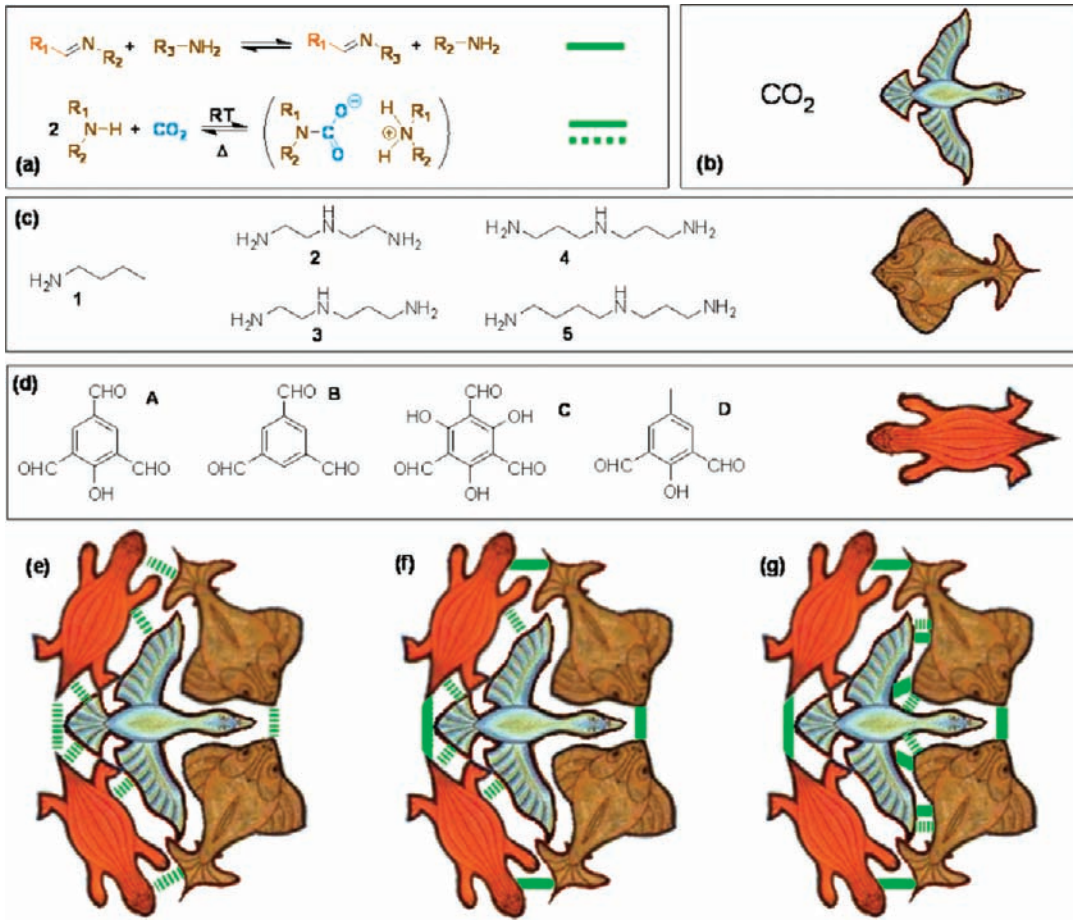

Figure 1. Top: building blocks and reversible linkages involved in the DCL for CO_2 capture: (a) transimination for oligomeric backbone formation and CO_2 capture by ammonium carbamate formation (b) CO_2 template (the "goose"), (c) polyamine **1**−**5** (the "fish") and (d) polyaldehyde **A**−**D** (the "turtle") building block. Bottom: host−guest self-assembly in DCC. (e) All noncovalent. (f) Covalent self-assembly induced by non covalent interactions with a template. (g) Mixing covalent and noncovalent template binding by a covalently assembled structure.

strategy to readily generate a wealth of architectures from simple building blocks through thermodynamically controlled self-assembly. In the absence of an external selector, one potential application of such a mixture called dynamic combinatorial library (DCL) is to identify, within pools of molecular objects, the most stable structure resulting from individual *intra*molecular or *inter*molecular noncovalent interactions between library members. Most often, a molecular partner is introduced to select species that act as hosts or receptors. In the latter case, while building blocks can self-assemble into molecular or supramolecular entities, the selection process of the host by the guest has so far been exclusively conducted by noncovalent means (Figure 1e and f, bottom). We herein report for the first time the implementation into the host−guest paradigm of DCC of a combination of covalent and noncovalent reversible interactions, respectively the carbamate and ammonium-carbamate linkages (Figure 1g).

Polyamines (Figure 1c) appeared as appropriate building blocks for exploring cooperative CO_2 binding and simultaneous imine exchange with carbonyl connectors. Secondary nitrogen sites can potentially be engaged into reversible ammonium carbamate linkage while primary ones should compete for CO_2 binding and imine exchange (Figure 1a). A characteristic feature of the C═N linkage is that its formation,[11a] substitution,[11b] and metathesis[11c] have all been reported to be under thermodynamic control in chosen conditions. Transimination in organic solvents[12a,b] in the absence of catalyst[12c] was selected to ensure rapid regulation of the composition and connectivity within the library during carbon dioxide introduction and subsequent ammonium carbamate formation. Preliminary experiments on model compounds confirmed that this exchange reaction was essentially isoenergetic and displayed faster kinetics than ammonium carbamate formation,[13] which should serve as the stimulus. While Schiff-base chemistry involving dicarbonyl species has been harnessed to provide numerous macrocyclic receptors in supramolecular chemistry,[14] we deliberately turned to tricarbonyl precursors (Figure 1d) to generate a wealth of

(10) (a) Lehn, J.-M. *Chem.—Eur. J.* **1999**, *5*, 2455–2463. (b) Lehn, J.-M.; Eliseev, A. V. *Science* **2001**, *291*, 2331–2332. (c) Rowan, S. J.; Cantrill, S. J.; Cousins, G. R. L.; Sanders, J. K. M.; Stoddart, J. F. *Angew. Chem.* **2002**, *114*, 938. *Angew. Chem., Int. Ed.* **2002**, *41*, 898−952. (d) Corbett, P. T.; Leclaire, J.; Vial, L.; West, K. R.; Wietor, J.-L.; Sanders, J. K. M.; Otto, S. *Chem. Rev.* **2006**, *106*, 3652–3711.

(11) (a) Huc, I.; Lehn, J.-M. *Proc. Natl. Acad. Sci. U.S.A.* **1997**, *94*, 2106–2110. (b) Giuseppone, N.; Lehn, J.-M. *J. Am. Chem. Soc.* **2004**, *126*, 11448–11449. (c) Oh, K.; Jeong, K. S.; Moore, J. S. *Nature* **2001**, *414*, 889–893.

(12) (a) Godoy-Alcantar, C.; Yatsimirsky, A. K.; Lehn, J.-M. *J. Phys. Org. Chem.* **2005**, *18*, 979–985. (b) Hutin, M.; Schalley, C. A.; Bernardinelli, G.; Nietschke, J. R. *Chem.—Eur. J.* **2006**, *12*, 4069–4076. (c) Giuseppone, N.; Schmitt, J.-L.; Schwartz, E.; Lehn, J.-M. *J. Am. Chem. Soc.* **2005**, *127*, 5528–5539.

(13) Caplow, M. *J. Am. Chem. Soc.* **1968**, *90*, 6795–6803.

(14) Borisova, N. E.; Reshetovo, M. D.; Ustynyuk, Y. A. *Chem. Rev.* **2007**, *107*, 46–79.

possible architectures (branched objects, macrocycles, capsules) from which CO_2 should select and amplify its best host. In particular, trialdehydes **A**−**C** and dialdehyde **D**[15] were chosen as connecting units between polyamines and were, prior to use, condensed with *n*-butylamine **1,** yielding building blocks $\mathbf{A1}_3$, $\mathbf{B1}_3$, $\mathbf{C1}_3$, and $\mathbf{D1}_2$ as transimination substrates (Figure 1). Upon exchange with polyamines **2**−**5**, the monoamine **1** released to solution should also serve as a traceable reporter of the extent of the transimination reaction in NMR spectroscopy.[16]

Results

To first determine whether branched, macrocyclic, or capsule architectures would be more suitable for CO_2 recognition, we generated a preliminary set of 16 libraries from simple pairs of cores and connecting units. In a typical experiment, monomer $\mathbf{X1}_n$ ($\mathbf{X} = \mathbf{A}-\mathbf{C}$, $n = 3$; $\mathbf{X} = \mathbf{D}$, $n = 2$) was combined with two equivalents of a triamine **2**−**5** in methanol at room temperature, yielding the DCL [**X**; ***n***]. The composition of the ensuing polyimine living solutions was analyzed by ^{1}H NMR and ESI(+)-MS spectrometry[17] comparatively before and after CO_2 introduction. Proton NMR confirmed that the resulting libraries differed from the initial components introduced and that *n*-butylamine **1** was released in the medium. ESI(+)-mass analysis showed that diversity in terms of sizes and topologies was indeed accessible from such precursors, although limited to objects up to dimers of the polyaldehyde core (capsules, macrocycles and branched adducts. See Figure 2). When CO_2 was introduced into these 16 living solutions, the resulting templated libraries [**X**; **n**; CO_2] remained homogeneous without any noticeable change in the repartition of the constitutive polyimine species, with the exception of $\mathbf{X} = \mathbf{A}$ and $\mathbf{n} = \mathbf{2}$ for which an abundant precipitate was obtained. In fact, although carbamates were formed and detected by NMR after CO_2 exposure, ^{1}H NMR and ESI(+)-MS revealed that this did not affect the transimination equilibria. Note that such adducts could only be detected by ESI-MS spectroscopy in negative mode when nonphenolic backbone **C** was used, presumably for ionization requirements (Supporting Information). For the combination (**X**; ***n***) = (**A**; **2**), the presence of carbamate species was confirmed by solid-state ^{13}C NMR spectroscopy.

This preliminary set of libraries was intentionally limited to a single building block belonging to the **X** and ***n*** family. Indeed, as each of these precursors displays multiple binding sites, the expected degree of accessible diversity shall grow exponentially with the number of building blocks, even within collections of low molecular mass objects. In the case of a symmetrical polyamine combined with a D_{2h}-symmetric aromatic core such as in the building block pair (**A**; **2**), imine−aminal tautomerism and phenol regioisomerism should generate a virtual combinatorial library[11a] of 120 members split into 12 different molecular masses, each of which was actually detected by ESI(+)-MS spectroscopy (Figure 2, top). Every remaining secondary or primary amine group on these oligomeric backbones is then available for either CO_2 binding or protonation, yielding of virtual collection of 2.77×10^4 possible objects in the templated system [**A**; **2**; CO_2] (Supporting Information). Introducing a dissymmetrical polyamine such as **3** or **5** alternatively to **2** or **4** multiplies by a factor of roughly 2^3, 2^4 and 2^5, respectively, the amount of expected aromatic monomers, macrocyclic and branched dimers (a dissymmetrical polyamine generates as much diversity as two symmetrical ones). As an illustration of this exponential growth, these templated libraries were estimated to contain about 7.22×10^5 members, although formed from three trivial but chemically different precursors (Figure 2, bottom).

As a noticeable exception in the [**X**; ***n***] series, because no amplification could be detected in the 15 other homologous mixtures, library [**A**; **2**] was highly perturbed by CO_2 introduction, quasi-quantitatively converting the network of scrambling soluble architectures into a solid ***S1*** (isolated yield: 90%). ^{1}H NMR (Figure 3) and, to a lesser extent, ESI(+)-MS analyses indicated that the supernatant was mainly constituted of *n*-butylamine carbamate with a few percent of the starting material $\mathbf{A1}_3$ and diethylenetriamine monocarbamate ($\mathbf{2}\cdot CO_2$). The solid precipitate ***S1*** proved to be insoluble in nonaqueous solvents (chlorinated, fluorinated, polar, coordinating, organic bases, and acids), and its dissolution in water was accompanied by imine hydrolysis and subsequent molecular scrambling. Despite our numerous attempts, no suitable macroscopic monocrystals could be obtained. Nevertheless, powder X-ray diffraction spectrum and peak widths in ^{13}C CP-MAS solid-state NMR revealed a high crystalline degree characterized by an elemental lattice of 9400 Å^3. *n*-Butylamine signals were absent from the NMR spectrum (Figure 4a.), indicating a complete displacement of the transimination equilibrium induced by CO_2 and the formation of a three-component material $[\mathbf{A}_x\mathbf{2}_y(CO_2)_z]_m$. CO_2 incorporation in this self-assembled system was confirmed by introducing $^{13}CO_2$ into the library [**A**; **2**], yielding a solid displaying the very same spectral signature, two peaks corresponding to usual carbamate chemical shifts[18] being clearly amplified (Figure 4a). Two-dimensional (2D) solid-state ^{15}N−^{13}C INEPT experiments revealed that, as expected, CO_2 was immobilized within the solid network through ammonium carbamate linkages (Figure 4d.).

To determine whether the main driving force of the process was the self-assembly of the solid adduct ***S1*** incorporating CO_2 or the favored formation of *n*-butylamine carbamate in solution,[5] a biased library excluding **1** and formed from 2-hydroxy-1,3,5-benzenetrialdehyde **A** and two equivalents of DETA **2** was forced to complete condensation by azeotropic distillation in a methanol/acetonitrile mixture. ESI(+)-MS analysis of this biased imination library revealed only two single detectable species: the capsule $\mathbf{A}_2\mathbf{2}_3$ and some remaining polyamine **2** due to the stoichiometry initially adopted ($n_0(\mathbf{A})/n_0(\mathbf{2}) = x_0/y_0 = 1/2$). As expected from a thermodynamically controlled system, this biased library transformed into [**A**; **2**] upon addition of 3 equiv of *n*-butylamine **1**. Similarly, when submitted to CO_2 uptake, this biased system yielded a solid ***S2*** which proved to be, from all solid-phase analyses aforementioned, identical to ***S1*** (Supporting Information). Conversely, desorption of CO_2 upon gentle refluxing of the methanolic suspension converted ***S1*** back to a homogeneous solution of $\mathbf{A}_2\mathbf{2}_3$ and **2**.

According to the reversible nature of the covalent self-assembling process, the solid structure should, in the presence

(15) (a) Anderson, A. A.; Goetzen, T.; Shackelford, S. A.; Tsank, S. *Synth. Commun.* **2000**, *30*, 3227–3232, 2000. (b) Temme, O.; Dickner, T.; Laschat, S.; Fröhlich, R.; Kotila, S.; Bergander, K. *Eur. J. Org. Chem.* **1998**, 651–659. (c) Chen, X.; Wang, J.; Sun, S.; Fan, J.; Wu, S.; Liu, J.; Ma, S.; Zhang, L.; Peng, X. *Bioorg. Med. Chem. Lett.* **2008**, *18*, 109–113. (d) Chong, J. H.; Sauer, M.; O'Brian, P.; MacLachlan, M. J. *Org. Lett.* **2003**, *5*, 3823–3826.

(16) (a) Leclaire, J.; Vial, L.; Otto, S.; Sanders, J. K. M. *Chem. Commun.* **2005**, 1959–1961. (b) Vial, L.; Ludlow, R. F.; Leclaire, J.; Perez-Fernandez, R.; Otto, S. *J. Am. Chem. Soc.* **2006**, *128*, 10253–10257.

(17) Gonzalez-Alvarez, A.; Alfonson, I.; Lopez-Ortiz, F.; Aguire, A.; Garcia-Granda, S.; Gotor, V. *Eur. J. Org. Chem.* **2004**, 1117–1127.

(18) Georges, M.; Weiss, R. G. *Langmuir* **2003**, *19*, 8168–8176.

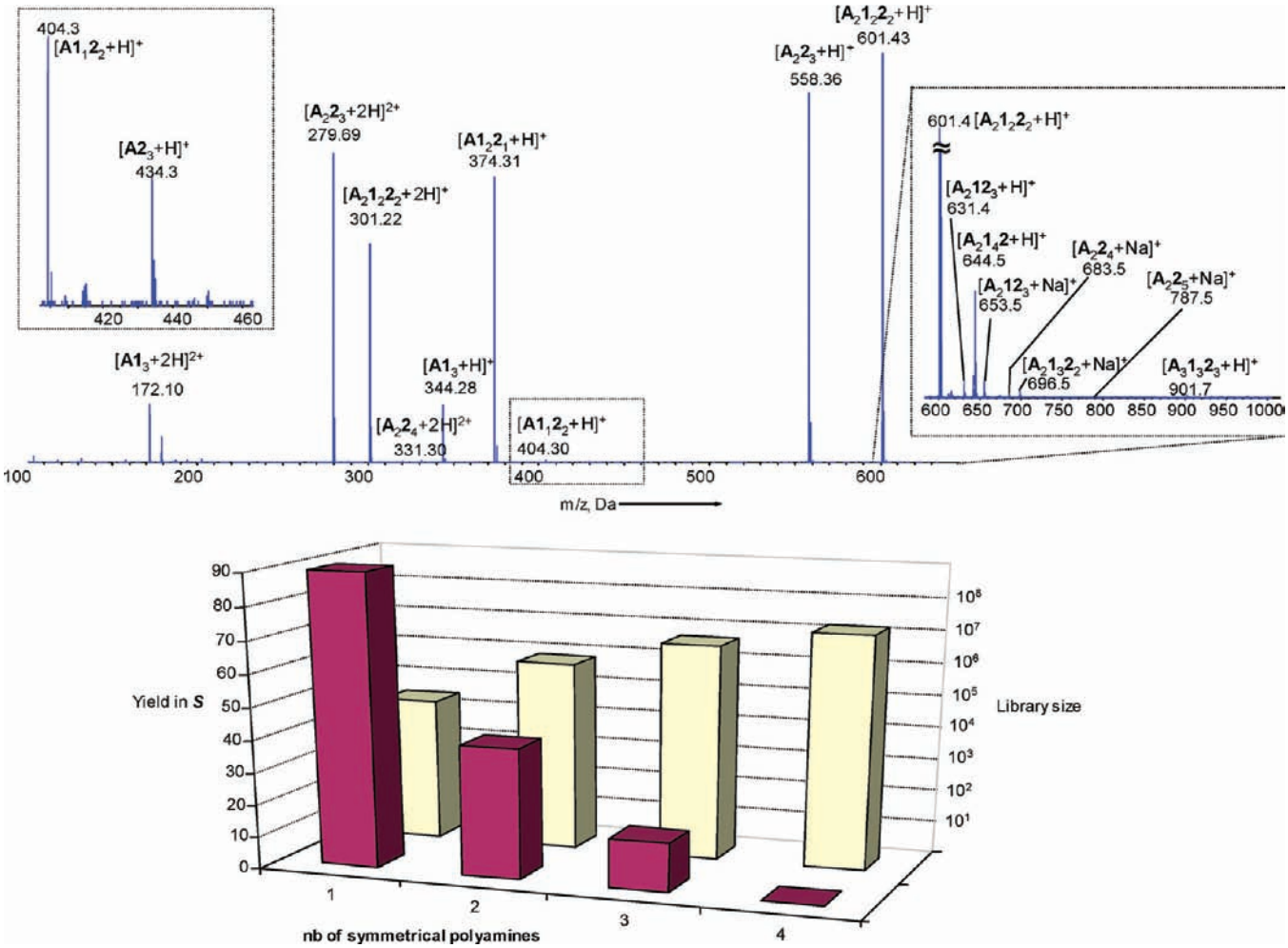

Figure 2. Top: ESI(+)-MS analysis of the untemplated library [**A**; **2**]. Bottom: correlation of the VCL size (yellow bars) and the yield in solid adduct ***S*** (purple bars) with the number of symmetrical polyamine spacers ***n***. Symmetrical−unsymmetrical pairs of polyamines are referred to as two symmetrical polyamines.

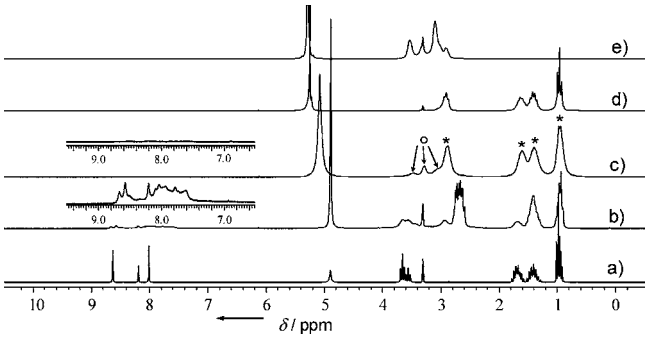

Figure 3. ^{1}H NMR (200 MHz) spectra of library [**A**; **2**] from (a) building block **A1**$_3$ (240 mM), (b) after transimination with 2 equiv of **2**, and (c) filtrate of the templated library [**A**; **2**; $\mathbf{CO_2}$]. * : [$\mathbf{1_2}$·CO_2] and ○ : [**2**·CO_2]. (d) ^{1}H NMR spectrum of [$\mathbf{1_2}$·CO_2] and (e) [**2**·CO_2] as references. Spectra were recorded at 300 K in CD_3OD.

of solvent, dynamically rearrange on both covalent and supramolecular levels upon CO_2 departure. The reversibility of carbon dioxide capture was confirmed by refluxing the heterogeneous methanolic suspension [**A**; **2**; CO_2] under a gentle nitrogen flow. Homogeneity was reached after several minutes. Proton NMR and ESI(+)-MS analyses confirmed return to the state of molecular diversity previously identified as [**A**; **2**] with undetectable hysteresis. Several cycles of absorption−precipitation/desorption−homogenization could be conducted according to this protocol, confirming that recycling was possible at moderate temperature (refluxing methanol) in the presence or in the absence of *n*-butylamine mother liquor, despite the formation of a highly organized solid network.[19]

Following those preliminary results, competition experiments between several polyamines were conducted under thermodynamic control to evaluate the constitutional specificity of the self-assembling process. Libraries [**A**; **2**; ***n***] (***n*** = **3** − **5**) were prepared and analyzed in the conditions described previously. ESI(+)-MS confirmed the expected increase in molecular diversity following the introduction of two polyamines (see Supporting Information). Templated libraries were estimated to reach up to 7.22×10^5 and 4.61×10^6 members respectively in the case of symmetrical−symmetrical and symmetrical−unsymmetrical pairs of polyamines ((**2**;**4**) and (**2**;**3**) or (**2**;**5**), respectively). In fact, symmetrical−unsymmetrical pairs generate as much diversity as three symmetrical polyamines (see Figure 2). Upon CO_2 exposure, every templated library produced a solid adduct with a yield that appeared to be correlated with

(19) In the presence or in the absence of *n*-butylamine carbamate mother liquor reconversion into the initial libraries respectively occurs in several minutes or more than half an hour, qualitatively illustrating the impact of the molecular diversity on the thermodynamic and kinetic parameters of the equilibria.

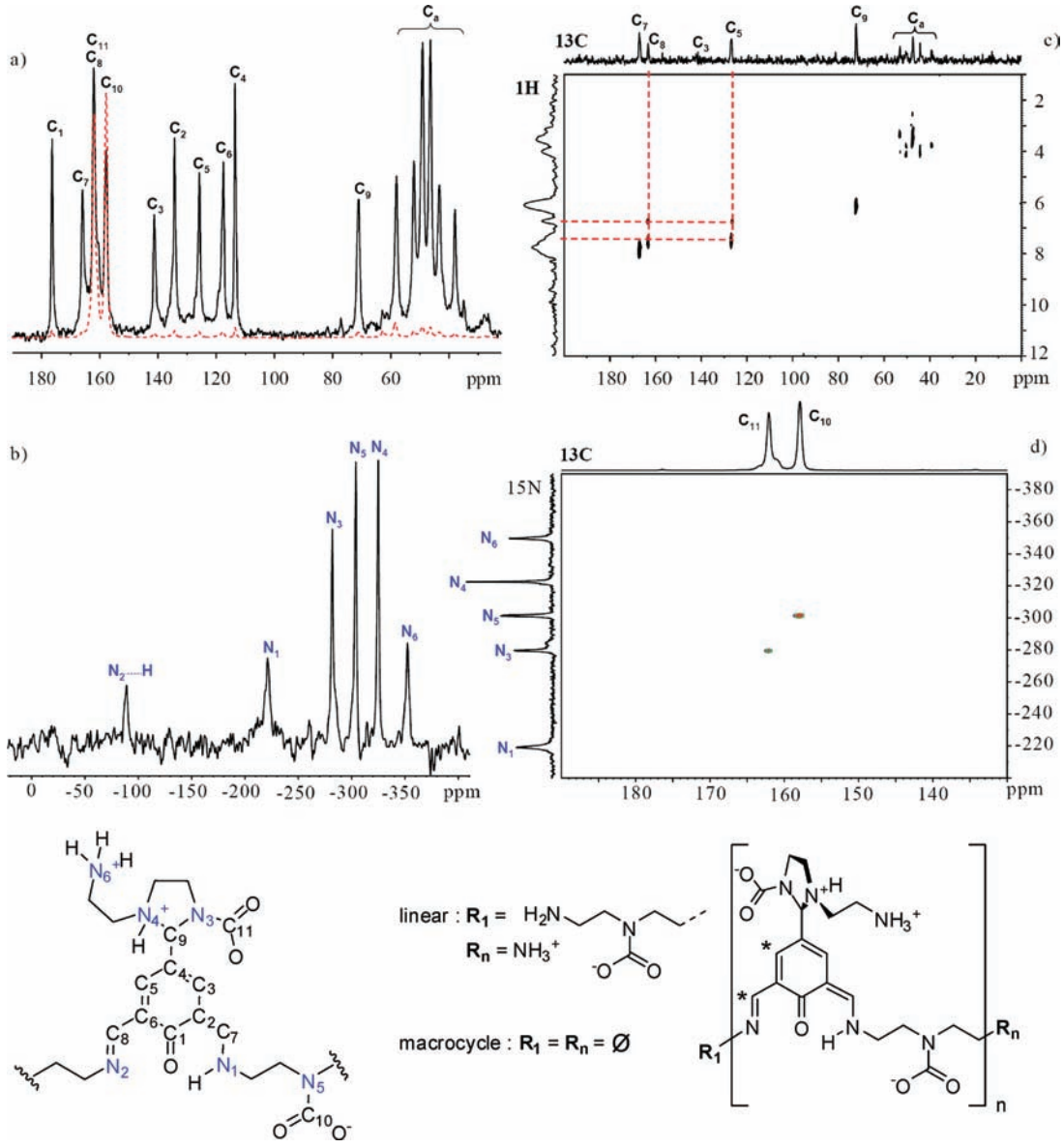

Figure 4. Multinuclear solid-state NMR attribution of the repeating unit constituting the solid ***S1*** (a) ^{13}C CP-MAS (dotted red line: from $^{13}CO_2$), (b) ^{15}N CP-MAS, (c) $^{1}H-^{13}C$ CP-MAS INEPT, and (d) $^{15}N-^{13}C$ CP-MAS INEPT. The presence or the absence of a DETA monocarbamate end group leads respectively to linear or cyclic oligomers. *: carbon atoms displaying two different $^{1}H-^{13}C$ correlations

the estimated degree of diversity (40% and 15% respectively for (**2**;**4**) or (**2**;**3**) and (**2**;**5**)). In each case, this adduct was identified in ^{13}C CP-MAS NMR analysis as the same material $[\mathbf{A}_x\mathbf{2}_y(CO_2)_z]_m$ having selectively and exclusively incorporated diethylenetriamine **2** at the expense of homologues **3**−**5** (Supporting Information). This result pointed out the exceptional constitutional selectivity of the system, allowing discrimination of the polyamine constituents differing by a single methylene unit. To further increase the diversity of the starting dynamic mixtures, libraries involving three competing polyamines [**A**; **2**; ***n***; ***n′***] were prepared. In the latter series, reaching a minimum estimated degree of diversity of 1.56×10^7 species (equivalent to 4 symmetrical polyamines. Figure 2), no solid adduct was obtained after CO_2 introduction.

The nature of the repeating monomeric unit within the material $\mathbf{A}_x\mathbf{2}_y(CO_2)_z$ was unambiguously identified using solid-state multinuclear NMR spectroscopy. ^{13}C CP-MAS experiments (Figure 4a) revealed a single type of constituting aromatic core. ^{13}C and ^{15}N (Figure 4b) chemical shift attributions revealed its substitution pattern was composed of an intramolecular enamine-quinone ion pair ($\delta N_1 = -221$ ppm),[20a] an imine hydrogen-bonded to a neighboring acceptor ($\delta N_2 = -89$ ppm),[20b] and an aminal group ($\delta N_4 = -325$ ppm; 1,3-dimethyl-2-phenyl-imidazolidine was synthesized as a reference compound for confirmation: $\delta N = -325$ ppm).[20c,d] Integration from direct ^{13}C solid-state NMR experiments provided an approximate repartition (x; y; z) = (1; 2; 2), with a degree of precision estimated to be about 10% from integration of reference compounds such as ethylenediamine monocarbamate, diethyenetriamine monocarbamate, and triethylenetetramine dicarbamate in the same conditions. These reference compounds also revealed that amine-

(20) (a) Schilf, W.; Kamiensky, B.; Kolodziej, B.; Grech, E.; Rozwadowski, Z.; Dziembowska, T. *J. Mol. Struct.* **2002**, *615*, 141–146. (b) Kamiensky, B.; Schilf, W.; Dziembowska, T.; Rozwadowski, Z.; Szady-Chelmieniecka, A. *Solid State Nucl. Magn. Reson.* **2002**, *16*, 285–289. (c) Clawson, J. S.; Anderson, K. L.; Pugmire, R. J.; Grant, D. M. *J. Phys. Chem. A* **2004**, *108*, 2838–2844. (d) Bera, M.; Wong, W. T.; Aromi, G.; Ray, D. *Eur. J. Inorg. Chem.* **2005**, 2526–2535.

to-carbamate conversion upon CO_2 capture systematically resulted in a 50 ppm downfield shift of the nitrogen center concerned. Consequently, ^{15}N signals $\delta = -281.8$ and -304.0 ppm were attributed respectively to the carbamates borne by N_3 and N_5, which was confirmed by 2D $^{15}N-^{13}C$ correlations[21a] (Figure 4d). As discussed in the following section, the only alternative would have been a carbamate linkage involving N_6. This scenario was excluded by simulations: as opposed to the previous scenario, it could not provide any packing mode that agreed with powder X-ray analyses. Two-dimensional $^{1}H-^{13}C$ spectrum revealed two types of through-bond correlations[21b] for C_5-H_5 and C_8-H_8, corresponding to two distinct aromatic rings with different magnetic environments. Such a subtle difference impacting the chemical shifts of H_5 and H_8 while leaving all carbon nuclei unaffected (Figure 4c) was attributed, in agreement with molecular analyses, to aromatic rings occupying a terminal or internal position on a linear oligomeric chain.

In fact, the identified monomeric unit can yield, through repetition, either macrocycles in the absence of end group or linear species when terminated by a diethylenetriamine monocarbamate unit (Figure 4, bottom). In addition to steric reasons, capsule structures appeared to be incompatible with such a constituting unit. The microcrystalline organization of the material and the observation of a single pair of minor and major monomeric aromatic units led to the conclusion that the number of covalent morphologies within ***S*** was reduced. Macrocyclic and branched/linear structural structures are indeed unlikely to coexist as isolated species or as combined units, i.e. within the material and within its constituting oligomers. Borohydride reduction of the templated heterogeneous systems [**A**; **2**; CO_2] was explored to provide some insight into the composition of the material. Analysis of the supernatant revealed a mixture of monomers and dimers of varying proportion with time. It is well-known that such a method, although frequently used to analyze homogeneous imine libraries,[22a] is valid provided that all members display the same reactivity toward reduction.[10d] The composition of the mixture shall therefore remain constant with time if reduction does not affect the scrambling reactions. In the present case, a small fraction of the solid adduct underwent disconnections−reconnections of its constituting labile linkages when suspended in methanol followed by subsequent solubilization of the fragments generated. The latter species are much more reactive toward hydrides than the solid network, which explains why only reduced objects of modest size could be detected. Moreover, while reduced capsules are unreactive toward polyimines, reduced branched and macrocyclic species carry primary amines that can take part in further transimination reactions. Similarly, freezing imine exchange in this heterogeneous dynamic combinatorial library with Ugi reaction[22b] led to the same observation and revealed that species differed in reactivity depending on their solubility. This difference resulted in altering the initial composition of the living mixture. More generally, these observations led to the conclusion that such methods are inappropriate for DCLs combining simultaneous phase-transfer processes (solid to liquid, liquid to gas) and possibly varying topologies (capsules, macrocycles, and branched objects). We alternatively turned to elemental analysis of the solid material, focusing on the nitrogen content as a key parameter to discriminate between the potential constituting structures. Unfortunately, no satisfying results were obtained despite rigorous screening of the combustion conditions. Carbon and nitrogen values remained incompatible with any type of structures and mixture of structures, whatever the amount of remaining solvent (methanol) or condensation side product (water) included in simulations (see Supporting Information). As reference compounds, pure carbamates of polyamines of increasing chain length evoked earlier were submitted to elemental analyses in the same conditions and revealed a noticeable and increasing deviation from the theoretical values, precluding the use of this method for a quantitative constitutional analysis.

Consequently, we decided to design a new set of experiments to precisely determine the composition of the self-assembled material. Constituting oligomers stacked in the solid phase resulted from two types of reversible and acid labile connections between three chemically distinct building blocks. Therefore, a complete disconnection combined with an independent titration of the resulting molecular fragments appeared as an attractive alternative to the analysis of the flash combustion products (elemental analysis). Acid hydrolysis in the presence of organic solvent[23] was followed by molecular ingredient quantizations using four complementary and routinely accessible techniques. The mass content in **A** was determined by UV titration. ^{1}H liquid NMR in the same hydrolytic conditions provided the building block ratio $x/y = n(\mathbf{A})/n(\mathbf{2})$ by integration. CO_2 content was determined by volumetric measurement, and TGA coupled to IR or MS led to the identification and quantization of a significant amount of water in the self-assembled polyzwitterionic material (Figure 5).

Although prepared using a trialdehyde/polyamine ratio of $y_0/x_0 = 2$, the material itself was characterized by a y/x stoichiometry of 2.22 ± 0.03, indicating a high content in polyamine-rich covalent structures such as linear/branched oligomers (Figure 5). Carbon dioxide and water content was evaluated to be respectively about 1 and 2 equiv per polyamine unit. The mass percentage of each of the different building blocks in the self-assembled material could be deduced independently of any hypothesis regarding the distribution of the oligomers and fitted the global mass of the solid analyzed with a precision of about 1%, noticeably superior to the precision obtained from elemental analyses.

To confirm the hypothesis of a distribution of oligomers within a material whose composition should be tuned by equilibrium displacement, the starting stoichiometry (y_0/x_0) was modified, and the resulting products were analyzed by the aforementioned multiple molecular titrations. Increasing the polyamine content with respect to the trialdehyde (from $y_0/x_0 = 2.10$ to 3.07) yielded materials ***S3***−***S5*** which, from solid-state NMR, powder X-ray diffraction, and elemental analysis appeared identical to ***S2.*** Building block titration revealed, as expected from a dynamic material, an increasing amount of polyamine (Figure 5) and consequently carbon dioxide with respect to the aromatic unit, through the formation of shorter constituting oligomers. Alternatively, ***S3***−***S5*** could be obtained by suspension of ***S2*** in methanol, thermal CO_2 desorption, addition of a controlled amount of polyamine, and reprecipitation upon CO_2 exposure.

(21) (a) Ramanathan, K. V.; Opella, S. J. *J. Magn. Reson.* **1990**, *86*, 227–235. (b) Elena, B.; Lesage, A.; Steuernagel, S.; Böckmann, A.; Emsley, L. *J. Am. Chem. Soc.* **2005**, *127*, 17296–17302.

(22) (a) Storm, O.; Lüning, U. *Chem.—Eur. J.* **2002**, *8*, 793–798. (b) Wessjohann, L. A.; Rivera, D. G.; León, F. *Org. Lett.* **2007**, *9*, 4733–6.

(23) Kanazawa, H.; Higuchi, M.; Yamamoto, K. *Macromolecules* **2006**, *39*, 138–144.

	Building block Analysis									Elemental Analysis		
	Stoechiometry (mmol/g)				Mass percentage (%)							
constituent / solid	A[a]	2[b]	CO_2[c]	H_2O[d]	A	2[e]	CO_2	H_2O	Total error[f]	C	H	N
S2	1.93 ± 0.01	4.28 ± 0.06	4.34 ± 0.03	7.99 ± 0.04	25.2	43.0	19.1	14.4	**1.6**	49.1 (45.9)	7.10 (7.10)	18.0 (17.7)
S4	1.81 ± 0.01	4.21 ± 0.06	4.29 ± 0.03	9.12 ± 0.04	23.5	42.3	18.9	16.4	**1.1**	48.6 (44.3)	6.97 (7.26)	18.2 (17.5)

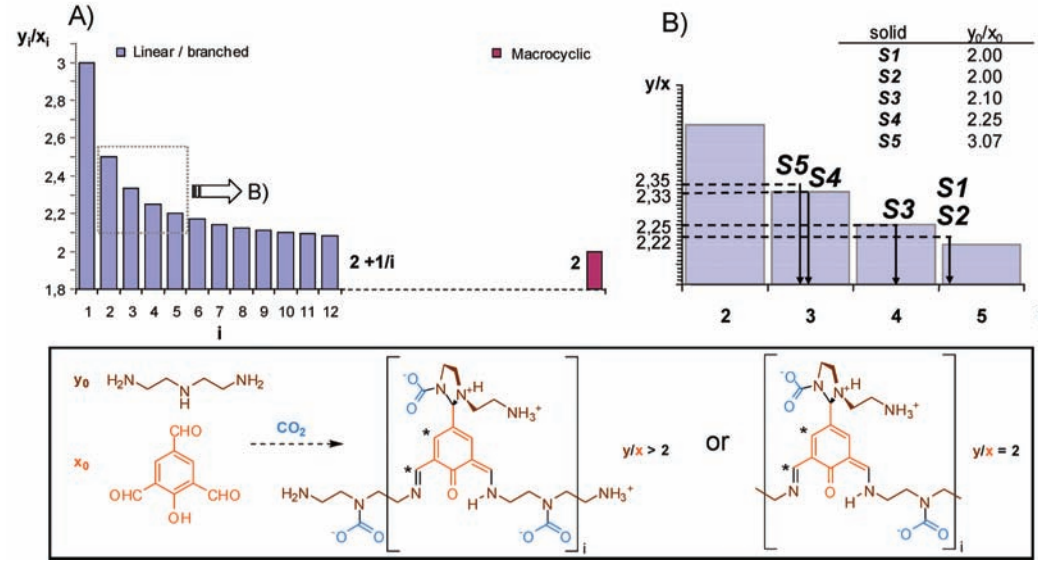

Figure 5. Table: Molecular (left) and elemental (right) analyses of self-assembled material $\mathbf{A}_x\mathbf{2}_y(CO_2)_z$ ***S2*** and ***S4***. For each material, analyses were run in triplicate on two samples prepared independently. (a) From UV titration at $\lambda = 340$ nm in $DMSO/H_2O/H_2SO_4$: 90:7:3. (b) ^1H integration at 500 MHz in DMSO-d_6/D_2O/D_2SO_4: 90:7:3. (c) Gasometric determination subsequent to hydrolysis with 6 M HCl. (d) From thermogravimetric analysis. (e) Independently of any hypothesis of distribution. (f) Calculated from $\Delta m/m$, Δm corresponding to the differences between the mass of the sample analyzed (m) and the individual mass contribution estimated by building block titrations. Bottom (A) Polyamine/aromatic core stoichiometries y_i/x_i for linear i-mers of **A** (bars) and macrocycles. (B) Horizontal dotted line: y/x ratios found for solids ***S1***−***S5***. Vertical dotted line: corresponding mean value of the distribution on the population restricted to linear 2- to 5-mer. Table: ratio y_0/x_0 used for the preparation of solids ***S1***−***S5***.

Interestingly, this disconnection method can be applied for the recovery of pure individual building blocks in the different phases (solid, liquid, gas) in a perspective of purification. Acidic hydrolysis of the solid material in pure aqueous medium is accompanied by the precipitation of pure **A** (the "turtle"), desorption of pure CO_2 (the "goose"), while diethylenetriamine **2** is solubilized as a salt and can be recovered as a pure liquid (the "fish") after flash chromatography on a DOWEX anion-exchange resin (see Figure 1 for building block classification). Such a result reveals that CO_2, through the constitutional selectivity of the self-assembling process, can be promoted as a precious auxiliary to purify **A** or **2** from polyaldehyde and polyamine mixtures. Conversely, **A** and **2** stand as selective agents to allow the purification of CO_2 from complex gaseous streams.

Due to the thermodynamic nature of the construction, CO_2 desorption should be considerably facilitated in the presence of the supernatant comparatively to nondynamic systems. As multiplying concurrent equilibria was proved to directly affect the yield of the self-assembling process, it is also likely to thermodynamically ease the expulsion of CO_2 from the solid material and its reconversion into an untemplated system of high molecular diversity. To a lesser extent, CO_2 desorption on the isolated self-assembled solid ***S*** should also compromise the stability and the molecular order of the whole network. In fact, as every building block contributes to the global stabilization of the molecular and supramolecular network, it is reasonable to expect that the first template molecule expulsed should yield a much less stable system, hence facilitating the departure of the following CO_2 molecules. Thermal characteristics of the isolated solids ***S*** were first studied by Differential Scanning Calorimetry, revealing three macroscopic endothermic events between 25° and 130 °C (about 75, 100, and 125 °C) (Figure 6). Thermogravimetry coupled to mass and infrared gas phase analysis on the one hand and variable temperature ^{13}C CP-MAS solid-state NMR spectroscopy on the other hand provided complementary microscopic information about the evolution of the composition of both the solid and gas phases with temperature. The first transition corresponded to the expulsion of the majority of the water content together with a few percent of carbon dioxide globally unaffecting the solid material and thereby providing a thermal treatment to dry the material without decomposition. The second transition (70−125 °C) was characterized by the simultaneous disappearance of the carbamate functionalities on the macromolecular backbone and detection of CO_2 in the gas phase. With a global heat of desorption of $\Delta H° = 15.7$ kJ/mol(CO_2), more than 95% of the carbon dioxide was expulsed during this event, followed by the departure of a few percent of remaining water and CO_2. The resulting glassy solid was characterized by a broad peak spectrum in ^{13}C CP-MAS NMR, indicating a complete loss of supramolecular organization consecutively to CO_2 departure (Supporting Information). As a contrast, ethylenediamine monocarbamate[24] was studied in the same conditions and underwent a unique and sharp (130−150 °C) thermal transition at 142 °C ($\Delta H° = 23.6$

(24) Gaines, G. L., Jr. *J. Org. Chem.* **1985**, *50*, 410–411.

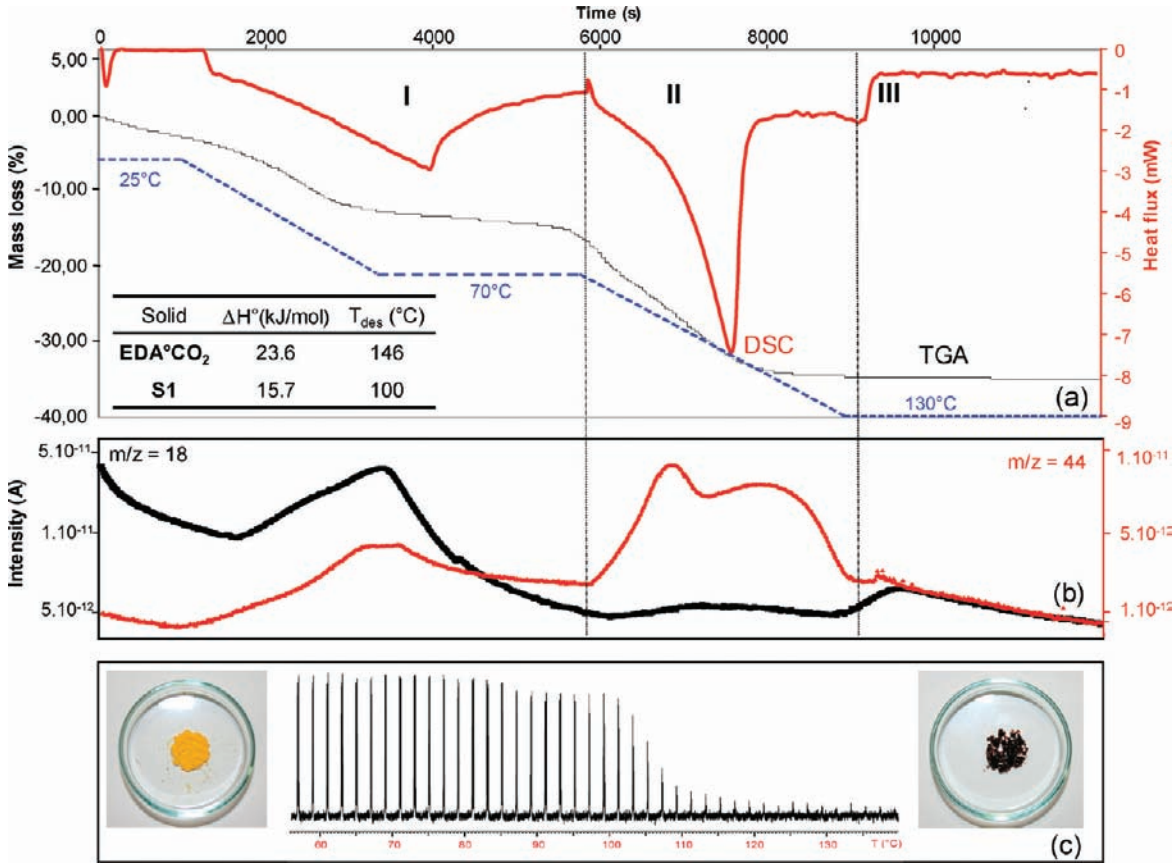

Figure 6. Thermal analysis of ***S1***. (a) Top: TGA (black) and DSC (red) curves corresponding to a sequential three-step thermal scan (blue dotted line). (b) Middle: total ion count at $m/z = 44$ and $m/z = 18$ corresponding to the main molecular peak of carbon dioxide and water. (c) Bottom: VT ^{13}C CP-MAS spectra focused on the carbamate multiplet ($158 < \delta < 164$ ppm) of the self-assembled material between (left photograph) 20 °C and (right photograph) 130 °C.

kJ/mol(CO_2)), corresponding to the sudden disappearance of the single carbamate signal in ^{13}C CP-MAS NMR (table in Figure 6).

Discussion

The results described above are evidence that simple building bocks (linear polyamines, tricarbonyl cores, and CO_2) displaying multiple sites for several reversible competitive connections (imine, aminal, and ammonium carbamate) can generate DCLs with complex network architectures from which original structures can be identified and isolated. In recent years, DCLs of increased architectural and compositional diversity have been explored, mostly by simultaneously utilizing several types of coupling chemistry for the construction of the libraries. Dynamic covalent bonds have been used in combination with orthogonal noncovalent,[25a,b] orthogonal labile covalent,[25c] or intricated covalent and noncovalent linkages.[25d] Some of us recently demonstrated that this approach could be extended to competitive reversible covalent linkages such as disulfides and thioesters.[16a] Within the frame of DCC, we managed herein to access a wide variety of topologies, each class including oligomers of modest but various sizes. When increasing the number of building block of one type and/or reducing their degree of symmetry, the number of constitutional homologues increased exponentially, providing straightforward access to large libraries from a very small set of precursors.

Nevertheless, simulations and experimental measures[26a] have recently proved that relative levels of amplifications may not necessarily be correlated with the binding affinities, especially when the size of the library is increased.[26b] A breakdown in the correlation may additionally occur when an excess of guest is used (here $p(CO_2) = 1$ represents an obvious stoichiometric excess)[27] and when several library members (trialdehyde and CO_2) compete for a scarce building block (the polyamine). These conditions were indeed all fulfilled in most of our soluble collections [**X**; ***n***; CO_2].

Our adaptative chemical system was designed to generate molecular receptors through a CO_2-driven shift in the distribution of the libraries' constituents toward the best binder. The selector being a gas in standard conditions, temperature and partial pressure were considered as potentially influencing the distribution of library members in solution. In this context of high molecular diversity and excess of gaseous template, no isolated molecular receptor could be identified in solution. Alternatively, our experimental conditions led to quantitatively and selectively obtaining a self-assembled three-component material as a

(25) (a) Kolomiets, E.; Lehn, J.-M. *Chem. Commun* **2005**, 1519–1521. (b) Sreenivasachary, N.; Lehn, J.-M. *Proc. Natl. Acad. Sci. U.S.A.* **2005**, *102*, 5938–5943. (c) Christinat, N.; Scopelliti, R.; Severin, K. *Angew. Chem., Int. Ed.* **2008**, *47*, 1848–1852. (d) Hutin, M.; Bernardinelli, G.; Nitschke, J. R. *Chem. Eur. J.*, **2008**, *14*, 4585–4593.

(26) (a) Corbett, P. T.; Sanders, J. K. M.; Otto, S. *Chem.—Eur. J.* **2008**, *14*, 2153–2166. (b) Corbett, P. T.; Otto, S.; Sanders, J. K. M. *Org. Lett.* **2004**, *6*, 1825–1827.

(27) (a) Saur, I.; Severin, K. *Chem. Commun.* **2005**, 1471–1473. (b) Corbett, P. T.; Sanders, J. K. M.; Otto, S. *J. Am. Chem. Soc.* **2005**, *127*, 9390–9392.

singularity among the building blocks screened. Its mass content in CO_2 reaches 20%, which approaches the loading capacity of monoethanolamine currently used in pilot plants (diluted in water, 20% massic, see ref 3). As previously described by Lehn et al. on linear chains[25a,b] and more recently by Iwasawa and colleagues on capsules,[28] obtaining a structured phase drives the selection of the components that make up the dynamic constituent producing the most highly organized and most stable assembly. The formation of an organized phase, not necessarily from the most stable covalent architecture, drives the selection process. This therefore explains the spectacular amplification obtained in the context of high molecular diversity, despite the use of an excess of CO_2.

The *combinatorial* screening provided by the dynamic combinatorial strategy yielded a structure−activity pattern of building blocks and molecular species that requires interpretation. In fact, the set of libraries analyzed revealed the compositional requirement for a stable self-assembled material: one set of building blocks appeared appropriate, and within the library thereby generated, one type of oligomer was amplified. This striking selectivity toward both the building blocks and the class of oligomers must then be exploited through a *Structure−Activity Relationship* approach to provide some potential insights into the highly favorable packing mode between the molecular constituents. As mentioned earlier, this efficient packing indeed constitutes the driving force and therefore the selector in the templating process. The substitution pattern of the aromatic unit, the length of the polyamine spacer, and the topology of the constitutive oligomers are discriminating criteria. Indeed, selection processes within soluble DCL generally favor small and cyclic objects for entropic reasons.[27b] The unexpected amplification of linear oligomers of high molecular masses (up to 2240 Da) should originate in their packing efficiency in the condensed phase. The substitution pattern (G_1, G_3, G_4, G_5) (Figure 7a) of the aromatic unit seems to essentially account for intramolecular oligomeric stabilization. In fact, the G_1 = OH substituent induces an imine−enamine tautomerism driven by an intramolecular stabilization, which is well-known on salicylic derivatives.[20a] Alternatively, the imidazolidine aminal cycle in the C4 position requires both the presence of a carbonyl group (G_4 = CHO) and the absence of sterically hindering substituents in C3 and C5 positions ($G_3 = G_5$ = H). This binding pattern is preferred to an imine linkage and therefore contributes to the stability of the oligomeric backbone. Interestingly, six-membered ring aminal cycles have been reported to be more stable than the corresponding five-membered analogues.[29] Therefore, polyamine selectivity favoring the shortest chain length that bears ethylene spacers presumably originates in the interoligomer noncovalent interactions. Among noncovalent interactions, ion pairs were shown from simulations to provide the main contributions in this polyzwitterionic material. Browsing crystallographic databases revealed that the X-ray structures of 2-phenylimidazolidine derivatives systematically display a common feature of fixed dihedral angle between the connected cycles, averaging 78° with a very sharp distribution.[30] Because ammonium centers are the only tetrahedral nitrogen sites, most of the conformational degrees of freedom in the three-dimensional structure of the oligomers are thus gathered in the aforementioned ethylene spacers. The bicyclic dihedral angle inevitably induces an intermolecular pairing along the *x* axis involving the primary ammonium-aminal carbamate (N_6-C_{11}; Figure 7a). Simulations on the alternative associations between tertiary aminal ammonium and aminal carbamate (N_4-C_{11}) never yielded any regular and efficient three-dimensional packing. This intermolecular binding mode was therefore ruled out. The remaining aminal ammonium-amine carbamate pairing appears to occur following a chelating pattern ($C'_{10}-N_4-C_{10}$) along the *z* axis. Such a binding mode requires an extended conformation of the bridging diethylenetriamine spacers, inducing an alternating *anti−anti* orientation of the aforementioned anionic−cationic−anionic binding sites on the same backbone. The relative positions of the aminal ring and the N_5-carbamate molecular moieties were herein defined as either *syn* or *anti* with respect to the $N_1(CH_2)_nN_5(CH_2)_{n'}N_2$ backbone (Figure 7a). These intermolecular binding modes and their conformational requirements provide a coherent and satisfying explanation of the polyamine selectivity experimentally observed. As expected from this model, building blocks **3**, **4**, and **5** should respectively yield *anti−syn*, *syn−anti*, and *syn−syn* orientations of the charged residues, each of which is unfavorable for intermolecular ion pairing along *z* and therefore precluding any efficient packing (Figure 7b, c, and d). This ionic binding mode along the *z* axis also underlines the importance of the third aldehyde function on the aromatic backbone for optimizing the intermolecular interactions. The electrostatic surface generated from the corresponding conformer of $\mathbf{A}_4\mathbf{2}_9(CO_2)_9$ reveals a "double comb" profile, confirming the electrostatic and steric self-complementarities along the *x* and *z* axes of this family of oligomers (Figure 7e). As an experimental confirmation of this proposed packing scenario, the volume of this envelope correlates finely with the dimensions of the crystal lattice determined from the powder X-ray spectrum.[31] Presumably, *y* axis interactions occur through the unpaired diethylenetriammonium carbamate-terminating groups acting as "sticky ends". This interpretative model provides a coherent picture of the structure-selectivity relationship of the system yielding, for a very single set of building blocks, as in Escher's famous symmetry drawing,[32] a three-component ("turtle−fish−goose") self-complementary class of oligomeric objects with unique packing ability (Figure 7f).

The *dynamic* facet of the combinatorial strategy provided a three-component system with unique and unexpected thermodynamic properties. As a critical concentration of the molecular precursors of the templated architecture should be reached to trigger the precipitation event, increasing the size of the library by introducing alternative building blocks produces an exponential number of new species competing for the selected constituents. This reduction in amplification predicted by simulations[27] is here embodied by the decrease in yield in ***S*** when the number of competing symmetrical polyamines is increased (90, 40, 15, and 0% obtained when introducing respectively 0, 1, 2, and 3 concurrent building blocks). Alternatively, converting back to a state of high molecular diversity [**A**; **2**] through reversible disconnection-reconnections thermodynamically facilitates the desorption step. In the pilot

(28) (a) Iwasawa, N.; Takahagi, H. *J. Am. Chem. Soc.* **2007**, *129*, 7754–5. (b) Takahagi, H.; Fujibe, S.; Iwasawa, N. *Chem.−Eur. J.* **2009**, *15*, 13327–30.
(29) Göblyös, A.; Lazar, L.; Fülhop, F. *Tetrahedron* **2002**, *58*, 1011–1016.
(30) Cambridge Crystallographic Database; 2009.
(31) Pepe, G.; Perbost, R.; Courcambeck, J.; Jouanna, P. *J. Cryst. Growth* **2009**, *311*, 3498–3510. The electrostatic envelope was estimated using the same genetic algorithm, GenMol.
(32) With courtesy of the M. C. Escher foundation: http://www.mcescher.com.

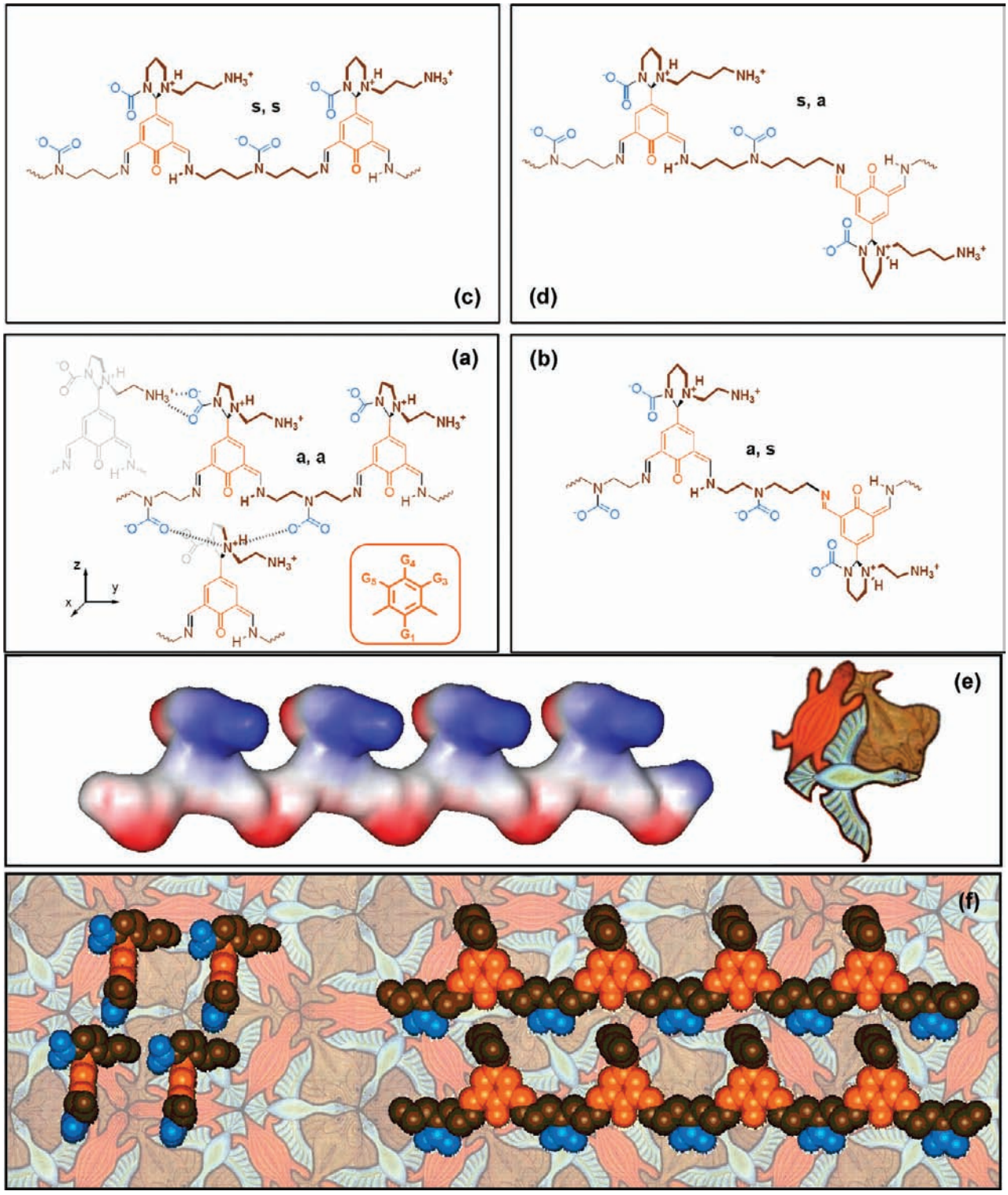

Figure 7. Top: Correlation between polyamine length and relative disposition of the ionic centers on a linear oligomer in extended conformation: (a) *anti*−*anti* for **2**, (b) *anti*−*syn* for **3**, (c) *syn*−*anti* for **4**, and (d) *syn*−*syn* for **5**. (e) Electrostatic surface of the corresponding oligomer $\mathbf{A}_4\mathbf{2}_9(CO_2)_9$ displaying a "double comb" profile and a self-complementarity for (f) efficient packing in the solid phase.

process CASTOR devoted to postcombustion capture currently tested,[3] this desorption step occurs through consecutive preheating of the amine aqueous solution and subsequent CO_2 stripping by a stream of vapor in a gas−liquid exchanger. Therefore, vapor generation and amine solution heating account for most of the energetic costs of the process. In this context, a decrease in the temperature required for CO_2 desorption comparatively to conventional molecular carbamates appears promising for rendering the process of "capture and release" economically attractive.[33] This reduction in the temperature of regeneration experimentally observed for [**A**; **2**] in refluxing methanol is partly explained by the "entropic" driving force consisting in multiple concurrent equilibria. It also accounts for the reduction in the yield of the most stable organized system during the

absorption step. Nevertheless, it could appear contradictory that the self-assembled material ***S*** should also be the most stable supramolecular pattern that can be obtained within the molecular network formed from three types of precursors. When the number of building blocks is limited to a polyamine such as **2** and CO_2, the complexity of the network is considerably lowered, and the most stable adduct is the molecular carbamate.[34] This entity may indeed be more stable than our self-assembled material but it does not form in the presence of an additional ingredient such as a polycarbonyl connector **A**. This modification of the molecular context explains the paradox that ***S*** can simultaneously be the best binder within the context of three-component systems (**A**/**2**/CO_2) while being less energy-demanding for recycling than a two-component adduct, such as a simple molecular ammonium carbamate (**2**/CO_2). The reduction of the free energy of the capture/regeneration step indeed occurs on both entropic and enthalpic bases. Reduction in enthalpy reaction is first due to the cooperativity of the process: carbamate bond-breaking/-forming is facilitated as the structure progressively dissociates or forms. Additionally, as mentioned earlier, the energetic levels of both the "untemplated starting resting state" (three reactants: **A** + **2** + CO_2) and the templated heterogeneous final system (**S**) are altered compared to a simple amine/CO_2 pair (undergoing the transmformation. **2** + CO_2 → **2**·CO_2). Hence, the gap between both states and the corresponding enthalpy of reaction is modified. Both entropic and enthalpic contributions impact the temperature of desorption in the liquid phase. Solid-phase analyses only illustrate the enthalpy-based cooperative self-assembly. In this particular case, the absence of mother liquor composed of solvent and concurrent amine(s) prevents any entropically- and enthalpically favored molecular scrambling that should yield the initial untemplated state of diversity [**A**; **2**] (Figure 6 photographs). Nevertheless, the synergistic nature of the three-component construction is well embodied by the desorption from the solid material displaying a broad and cooperative transition, as opposed to molecular carbamates. As a result of this synergy, the temperature of desorption drops from 140 to 100 °C, and the corresponding average heat is lowered by a factor of 0.65 which, as mentioned earlier, only accounts for a fraction of the total reduction expected in the liquid phase.

Beyond the proof-of-concept that CO_2 may be used as a building block in DCC, implementing system chemistry in the paradigm of CO_2 capture seems to be a promising route toward the reduction of the costs of capture, showing how interactions between molecules lead to the emergence of a cooperative behavior.[35] This process may one day become economically more attractive than direct emission. Such a multicomponent strategy also reveals that carbon dioxide can be promoted as a synthetic auxiliary and building block, giving access to adaptative, recyclable, and architecturally complex materials. Providing a complete molecular picture of the self-assembly in the solid phase proved a challenging task. Solid-state NMR allowed us to identify the main repeating molecular unit formed from the three building blocks **A**, **2**, and CO_2. As an alternative to elemental analysis, building block titration appeared as a straightforward and powerful method of analysis of multicomponent dynamic materials. This new analytical approach allowed us in some ways to straddle two rather different areas: that of discrete molecular species, where the traditional tools of analysis are usually available, and that of polymer chemistry, where rather different tools are applied and with different goals. It unambiguously provided the length and topology of the constitutive oligomers obtained by the repetition of the identified monomeric unit. Such a disconnection strategy, based on the reversible nature of the construction, leads to two essential observations. Building blocks can thereby easily be recovered as pure compounds, promoting CO_2 as a valuable and green auxiliary for the purification of polyamine and polyaldehyde from homologous mixtures. Additionally, modulating the building block stoichiometry results in finely tuning the constitutive population of self-assembled covalent oligomers within a structural family (centered here between linear dimers and pentamers). More importantly, the loading capacity can thereby be modulated within what appears to be a new type of adaptative and recyclable organic material.

Methods

Generation of Combinatorial Libraries. In a typical experiment, a di- or tributylimine core (0.182 mmol; $\mathbf{A1}_3$: 62.6 mg; $\mathbf{B1}_3$: 59.7 mg; $\mathbf{C1}_3$: 68.3 mg; $\mathbf{D1}_2$: 50.0 mg) is diluted in methanol (10 mL). Two equivalents of triamine ***n*** (0.365 mmol) or of an equimolar mixture of triamines are then added, and the clear yellow solution is stirred at room temperature for 30 min, yielding library [**X**; ***n***; ***n′***]. CO_2 is then introduced by gentle bubbling for 15 min (during which precipitation occurs in the case (**X**, ***n***) = (**A**, **2**)), yielding library [**X**; ***n***; ***n′***; CO_2]. At this stage, nitrogen can be introduced by gentle bubbling while refluxing the resulting solution for 30 min for complete CO_2 desorption (yielding library [**X**; ***n***; ***n′***]).

Material $\mathbf{A}_x\mathbf{2}_y(\mathbf{CO_2})_z$. From Library [A; 2]. CO_2 is introduced by gentle bubbling for 15 min, during which precipitation occurs, yielding library [**A**; **2**; CO_2]. ***S1*** can be isolated: the heterogeneous solution is centrifuged and filtered. The resulting pale-yellow solid is then washed with methanol (2 × 5 mL) and dried under vacuum pressure. It can be further dried by heating at 70 °C under nitrogen flux for 1 h.

From Direct Imination Library. In a typical experiment, 2-hydroxy-1,3,5-benzenetricarbaldehyde **A** (0.182 mmol; 32.4 mg) and diethylenetriamine **2** (***S2***: 0.365 mmol; 37.7 mg. ***S3***: 0.383 mmol; 39.6 mg. ***S4***: 0.411 mmol; 42.4 mg. ***S5***: 0.560 mmol; 57.9 mg) are dissolved in an acetonitrile−methanol mixture(4 + 8 mL) in a RB-flask equipped with Dean−Stark apparatus. The acetonitrile−methanol−water ternary azeotrope is continuously distilled for 4 h while fresh methanol is reintroduced every 15 min, keeping the concentration constant. After cooling back to room temperature, CO_2 is bubbled in the solution until precipitation is complete. Purification is accomplished by using the the previous procedure.

Yield: 90%; ^{13}C NMR: 177.6 (C−OH), 167.1 (CH=NH^+), 163.2 (CH=N), 163.2 (N−COO−), 159.1 (N−COO−) 142.5 (CH=C), 135.4 (C=C), 127.1 (CH=C), 118.7 (C=C), 114.6 (C=C), 72.3 (N−CH−N), 59.2 (CH_2−N), 53.2 (CH_2−N), 50.3 (CH_2−N), 47.5 (CH_2−N), 44.3 (CH_2−N), 39.0 (CH_2−N); ^{15}N NMR: −89.0 (CH=N), −221.4 (CH=NH^+), −281.8 (N), −304.0 (N), −325.0 (N, NH), −352.4 (NH_3^+); decomposition (DSC): 70.6, 101.6, 125.7 °C.

Poly(*n*-butyl)imine Cores Synthesis. Di- or trialdehyde (3.12 mmol) (2-hydroxy-1,3,5-benzenetricarbaldehyde: 0.55 g; 1,3,5-benzenetricarbaldehyde: 0.51 g; 2,4,6 trihydroxy-1,3,5-benzenetricarbaldehyde: 0.66 g; 2-hydroxy-5-methyl-1,3-benzenedicarbaldehyde: 0.51 g) and *n*-butylamine **1** ($\mathbf{A1}_3$: 0.98 g; 13.42 mmol; $\mathbf{B1}_3$: 0.98 g; 13.42 mmol; $\mathbf{C1}_3$: 0.98 g 13.42 mmol; $\mathbf{D1}_2$: 0.65 g; 8.91 mmol)) are diluted in a suspension of 4 Å molecular sieves in

(33) European Climate Exchange: http://www.ecx.eu.
(34) This adduct is unfortunately liquid at room temperature and therefore could be used as a reference in the set of thermal solid-phase analyses.
(35) Nitschke, J. R. *Nature* **2009**, *462*, 736–8.

THF (10 mL). The mixture is refluxed for 19 h after which the solution is cooled to room temperature and filtered. The solvent is removed by evaporation and the residual *n*-butylamine by distillation under reduced pressure.

Summary

As a proof of concept, a dynamic combinatorial selection approach has provided a self-assembled multicomponent organic material incorporating carbon dioxide, depicting selectivity for the constitutional building blocks required down to one carbon unit and paving the way toward a promising reduction of energetic costs of recycling.

Acknowledgment. We thank Dr. V. Heresanu for powder X-ray diffraction, Dr. Benedicte Elena for 2D $^{1}H-^{13}C$ NMR analysis, and Dr. G. Pepe for preliminary calculations. Financial support from the TGE RMN THC and IFP for conducting the research is gratefully acknowledged.

Supporting Information Available: Experimental procedures, characterization data for all new compounds and libraries, and evidence for dynamic interconversion of $\mathbf{A}_x\mathbf{2}_y(CO_2)_z$.This material is available free of charge via the Internet at http://pubs.acs.org.

JA909975Q